Materials Science Forum Vols. 258-263 (1997) pp. 515-520
online at http://www.scientific.net
© (1997) Trans Tech Publications, Switzerland

IDENTIFICATION OF VH IN SILICON BY EPR

P. Johannesen[1], J. R. Byberg[2], B. Bech Nielsen[1], P. Stallinga[1], and K. Bonde Nielsen[1]
[1] Institute of Physics and Astronomy, University of Aarhus, DK-8000 Århus C, Denmark.
[2] Institute of Chemistry, University of Aarhus, DK-8000 Århus C, Denmark.

Keywords: Silicon, vacancies, hydrogen, dangling bonds, EPR, point defects, electronic properties.

Abstract
Floatzone grown silicon crystals have been implanted with protons or deuterons. Electron Paramagnetic Resonance (EPR) spectra show the presence of a strongly temperature dependent signal in addition to the well-known S1 signal. The temperature dependent signal displays monoclinic-I symmetry below 65 K and trigonal symmetry above 110 K. The g- and ^{29}Si hyperfine tensors are characteristic of defects with the unpaired electron confined mostly to a dangling bond orbital in a vacancy-type defect. The signal shows splittings arising from the hyperfine interaction with a single proton. On this basis, and from the close similarity with the familiar VP^0 signal (the E-center), we conclude that the signal originates from VH^0, the neutral charge state of the silicon monovacancy containing a single hydrogen atom.

Introduction
The continued search for the detailed structures of hydrogen-related point defects in crystalline silicon is essential to our understanding of how hydrogen modifies the electronic and optical properties of silicon. Furthermore, experimentally determined structures of such defects constitute an excellent testing ground for *ab initio* calculations. Although the properties of hydrogen in silicon have been intensively studied during the past decade [1], few defect structures involving hydrogen have been established [2, 3, 4, 5]. The present work offers the identification of a fundamental hydrogen-related point defect in silicon, the existence of which has been expected for more than a decade.

In molecular compounds, such as SiH_4, hydrogen and silicon form strong covalent bonds. Therefore, any defect that may form such bonds constitutes a deep trap for hydrogen. The monovacancy is such a structure. Bech Nielsen *et al.* [5] found direct evidence of this in a study of the local vibrational modes of point defects in proton-implanted silicon by FTIR (Fourier Transform InfraRed) spectroscopy. They identified the Si-H stretch modes of VH_2, VH_3 and VH_4, that is, monovacancies binding two, three and four hydrogen atoms, respectively. Thus the existence of vacancy-hydrogen complexes in silicon has been established, but the electronic properties of these defects remain to be determined experimentally. Furthermore, VH, the simplest member of this series of defects, has not yet been identified.

The expected structure of VH^0, the EPR-active neutral charge state of VH, may be deduced from a simple LCAO picture: Introducing a vacancy in the silicon lattice creates four free sp^3 hybridized silicon orbitals, one of which forms a strong covalent bond with the hydrogen atom. The one-electron energies of the bonding and antibonding combinations of the silicon orbital and the hydrogen 1s orbital lie well below the top of the valence band and well above the edge of the conduction band, respectively. This is due to the large ionization potential of hydrogen and to the strong overlap of the two orbitals. The presence of the hydrogen atom changes the symmetry of the unrelaxed vacancy from T_d to C_{3v}. The remaining three silicon orbitals form a bonding combination belonging to the symmetric representation A with energy well below the top of the valence band and a pair of degenerate combinations belonging to the representation E with energy within the band gap.

All rights reserved. No part of contents of this paper may be reproduced or transmitted in any form or by any means without the written permission of the publisher: Trans Tech Publications Ltd, Switzerland, www.ttp.net. (ID: 193.136.225.10-02/10/06,11:23:55)

In the neutral charge state of VH the E level is singly occupied leading to a Jahn-Teller distortion from C_{3v} to C_{1h} symmetry. Hence two of the silicon orbitals are expected to combine, forming a reconstructed bond, while the remaining silicon orbital is left as a singly occupied dangling bond that contains most of the unpaired electron spin density. According to this description, VH^0 should have monoclinic-I symmetry with the dangling bond and the Si-H bond pointing almost in ⟨111⟩ directions in a {110} mirror plane. This structure, depicted in Fig. 1, is consistent with the results of *ab initio* calculations [6, 7].

Since the structure sketched above corresponds closely to that of VP^0 (the E-center) [8], in which a substitutional phosphorus atom is located next to a monovacancy, it may be expected that the electronic properties of VH^0 resemble those of VP^0.

In this paper we report the identification of VH^0 in proton-implanted silicon. The observed properties, including the electron spin distribution, the hydrogen hyperfine interaction and a thermally activated change of the effective symmetry, all corroborate the model of VH^0 and testify to the close similarity with VP^0.

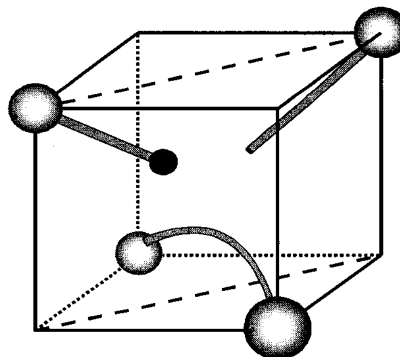

Figure 1. The model of VH^0 showing the vacancy in the center, the Si-H bond and the dangling bond in the {110} mirror plane, and the reconstructed bond perpendicular to the plane.

Experimental

The samples were n-type (resistivity: 600 Ωcm) silicon crystals grown by the floatzone technique. The concentration of phosphorus was $\sim 9\times10^{12}$ cm^{-3}, while the concentration of other impurities, mainly oxygen and carbon, was below 3×10^{16} cm^{-3}. Slabs measuring 1×3×4 mm^3 were cut with the large faces perpendicular to a {110} plane. After polishing, both large faces were implanted with protons (or deuterons) at 56 (or 38) successive energies in the range from 5.3 to 10.5 MeV (or 5.0 to 10.6 MeV). The dose implanted at each energy was calculated to ensure a uniform distribution of hydrogen throughout the sample corresponding to a concentration of $\sim 4\times10^{17}$ cm^{-3}. During the implantation, the sample temperature was kept below 120 K. The samples were subsequently warmed to room temperature and etched in nitric and hydrofluoric acid to remove surface defects that might be EPR active.

The experimental setup consists of a Bruker ESP300E spectrometer operating in absorption mode at X band (~9 GHz) and Q band (~34 GHz). EPR spectra were recorded at 5° intervals in the $(1\bar{1}0)$ plane. The static magnetic field $\mathbf{B_0}$ was monitored with a resolution of 1 μT with a Bruker ER-035 NMR gaussmeter. Resolution enhancement by third harmonic detection [9, 10] was employed: The magnetic field was modulated at 33 kHz with a small admixture of 100 kHz, and the EPR signal was lock-in detected at 100 kHz. By adjusting the amplitudes of the 33 and 100 kHz modulations correctly, a decrease in linewidth of ~30 % could be obtained without introducing spurious lines. The sample was placed in a liquid helium cryostat allowing its temperature to be controlled in the range from 10 K to 300 K. Isochronal (20 minutes) annealing of the samples was done in steps of 15°C with a controlled flow of heated nitrogen gas.

Results

In addition to the S1 signal, previously observed in EPR spectra of proton-implanted silicon crystals [11], our EPR spectra contain a new, strongly temperature dependent signal which we label vh^0, anticipating the identification with the VH^0 defect made below. The spectrum of the deuterium implanted sample Si:D recorded with $\mathbf{B_0}$ || [111] at different measurement temperatures is shown in

Fig. 2. At the microwave power employed, the S1 signal becomes partially saturated below 85 K, which makes it possible to separate out the vh^0 signal. At 45 K, vh^0 consists of the three lines *A*, *B* and *C* (line *A* almost coincide with one of the lines of S1). As the temperature is raised, *A* and *B* begin to broaden and finally disappear at 85 K, while *C* persists. Above 110 K a new line *AB* emerges at a position dividing the distance from *A* to *B* in the ratio 1:2. It attains a maximum in intensity (and a minimum in linewidth) at 145 K. At higher temperatures both *C* and *AB* broaden, becoming undetectable at room temperature. An isochronal annealing study confirmed that *A*, *B*, *C* and *AB* originate from the same defect, which anneals out at ~480 K.

Spin-Hamiltonian terms		VH^0	VP^0
$\underline{g}$ (± 0.0001)	X	2.0090	2.0096
	Y	2.0114	2.0112
	Z	2.0006	2.0005
	θ	32.4°	32°
$\underline{A}(^{29}Si)$ (MHz) (± 1 MHz)	X	-275	-295
	Y	-275	-295
	Z	-435	-450
	θ	35.3°	35.3°
$\underline{A}^H$ (MHz) (± 0.3 MHz)	X	-3.3	
	Y	-4.6	
	Z	8.5	
	θ	8°	

Table I. The spin Hamiltonian parameters for vh^0 at 45 K and for VP^0 [8]. The principal axis Y is parallel to the $[1\bar{1}0]$ axis, while X and Z span the $(1\bar{1}0)$ plane, Z making the angle θ with the [110] axis. The quoted uncertainties pertain to vh^0.

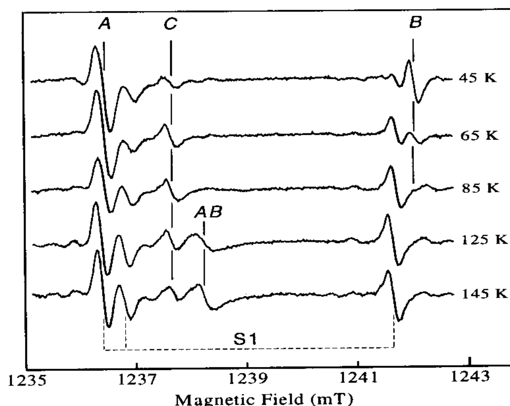

Figure 2. Spectra of Si:D recorded at different sample temperatures with $\mathbf{B_0}$ along [111] and at 34.778 GHz. The lines *A*, *B*, *C* and *AB* belong to the signal vh^0.

The temperature dependence of vh^0 in the region 45-145 K suggests that the corresponding defect undergoes a thermally induced symmetry change. This is confirmed by the angular variation of vh^0 in the $(1\bar{1}0)$ plane for Si:D, which is shown in Fig. 3: The g tensor shows monoclinic-I symmetry at 45 K (open circles) and trigonal symmetry at 145 K (filled circles).

Direct evidence of the incorporation of hydrogen in the defect responsible for vh^0 is obtained by a comparison of the spectra of Si:H and Si:D: Fig. 4 shows corresponding spectra recorded at 45 K with $\mathbf{B_0} \parallel [110]$; the four lines belonging to vh^0 in Si:D are labelled by *D* through *G*. The lines *D* and *G* appear as doublets in Si:H, whereas the lines *E* and *F* appear at the same positions in Si:D and Si:H. The doublet splittings in Si:H reveal the involvement of a single hydrogen atom in the defect, while the absence of resolved splittings of *E* and *F* indicates that the hyperfine interaction is strongly anisotropic. The spectra may be represented in terms of the spin Hamiltonian

$$H_{spin} = \beta\ \mathbf{S}\underline{\mathbf{g}}\mathbf{B}_0 - g_p\beta_n\ \mathbf{I}\cdot\mathbf{B}_0 + \mathbf{S}\underline{\mathbf{A}}^{\mathbf{H}}\,\mathbf{I}$$

where g_p is the g value of the proton, and β and β_n are the Bohr- and nuclear magneton, respectively. The principal values of $\underline{\mathbf{g}}$ and $\underline{\mathbf{A}}^{\mathbf{H}}$, describing the hyperfine interaction with the hydrogen nucleus, are listed in Table I, and simulations of the signals for $\mathbf{B_0} \parallel [110]$ calculated from these parameters are shown in Fig. 4 as dashed curves. The nuclear Zeeman energy of the proton at the magnetic fields employed is much larger than the proton hyperfine interaction, implying that the splittings observed *between* the principal directions of $\underline{\mathbf{A}}^{\mathbf{H}}$ depend strongly on the relative signs of the principal values. Hence these signs could be determined unambigously. The deuteron hyperfine

splittings calculated from the observed proton splittings are smaller than the linewidth for all orientations of $\mathbf{B_0}$ in accordance with the absence of resolved splittings in the signal observed in Si:D.

In the spectra recorded below 65 K of both Si:D and Si:H, we observe a pair of weak satellites belonging to each of the main lines. The relative intensitiy of each pair of satellites is ~2 %, and the splitting between a pair of satellites is independent of the microwave frequency. We therefore ascribe these satellites to the hyperfine interaction with the ^{29}Si nucleus of *one* nearby silicon atom. The corresponding hyperfine tensor has trigonal symmetry (Table I). Hyperfine interactions with other silicon nuclei in the vicinity of the defect were not resolved.

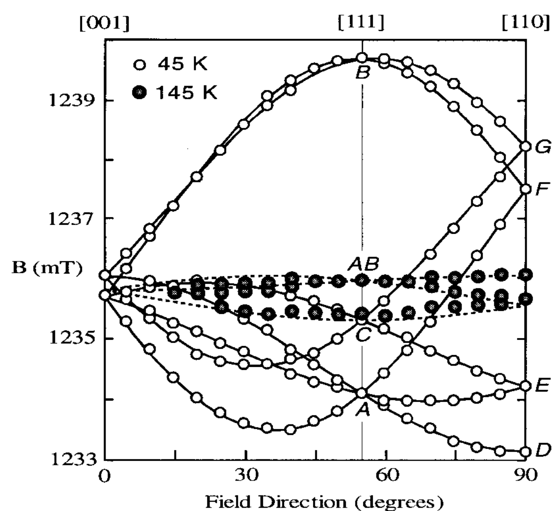

Figure 3. The angular dependence of vh^0 in the $(1\bar{1}0)$ plane at 34.710 GHz for Si:D. The open and filled circles indicate measurements at 45 K and 145 K, respectively. The solid curves are calculated from the g tensor in Table I, and the dashed curves are calculated from the motional average of this tensor (see text). Labels at $B_0 \parallel [111]$ refer to Fig. 2, while labels at $B_0 \parallel [110]$ refer to Fig. 4.

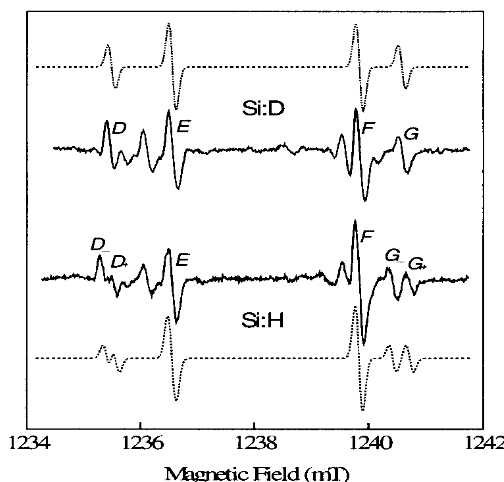

Figure 4. Spectra (solid curves) of Si:D and Si:H recorded at 45 K and 34.777 GHz with $\mathbf{B_0}$ along [110]. The labelled lines belong to vh^0. The dashed curves represent simulations based on the parameters in Table I.

Analysis and discussion

The g tensor representing the low temperature form of vh^0 has monoclinic-I symmetry and is nearly axial ($g_X \approx g_Y$) with its unique axis Z deviating only 3° from the [111] axis (Table I). According to the classification scheme of Lee and Corbett [12], such a g tensor is typical for centers in which the unpaired electron is largely confined to a dangling bond orbital in a vacancy-type defect. A simple LCAO analysis of the observed hyperfine interaction with a single ^{29}Si nucleus suggests that 54 % of the electron spin is located on the silicon atom in an orbital with 13 % s-character and 87 % p-character. These values are typical for dangling bonds around vacancies [12]. From Table I it can be seen that $\underline{\mathbf{g}}$ and $\underline{\mathbf{A}}(^{29}Si)$ of vh^0 closely resemble the corresponding parameters of VP^0. This indicates that the structure and distribution of electronic spin of the defect associated with the vh^0 signal are very similar to those of VP^0.

Combining this result with the observation of a hyperfine interaction with one proton, we may conclude that the defect consists of one or several vacancies binding a single hydrogen atom. The number of vacancies involved may be inferred from the magnitude of the proton hyperfine interaction: We note that the isotropic hyperfine constant a = $^1/_3$ ($A_X + A_Y + A_Z$) is only 0.2 MHz (Table I) indicating a negligible spin density at the proton. We may therefore ascribe the observed anisotropic hyperfine splitting to the dipolar interaction of the proton spin with the electron spin confined essentially to the dangling bond orbital. Within the point dipole approximation, the distance R between the proton and the silicon atom carrying the dangling bond may be estimated from the expression $b = g_e\beta\, g_p\beta_n\, R^{-3}$ with b = $^1/_6$ ($2A_Z - A_X - A_Y$) = 4.1 MHz (Table I). The result is R = 2.7 Å, in excellent agreement with the value of 2.8 Å calculated from the unrelaxed geometry of VH^0 with the 1.5 Å Si-H bond pointing exactly in a ⟨111⟩ direction. A similar calculation for the unrelaxed geometry of the divacancy binding a single hydrogen atom (V_2H^0) yields R = 4.7 Å. These values strongly indicate that vh^0 originates from VH^0 rather than from V_2H^0. Scaling R with the ratio of the lattice constants of diamond and silicon yields R = 1.8 Å for VH^0 in diamond, in accordance with the value of 1.9 Å derived for the H1 defect in diamond [13], the structure of which is believed to resemble that of VH^0.

The identification of the defect responsible for vh^0 with the neutral charge state of the silicon monovacancy containing a single hydrogen atom gains additional support from the observed transition from monoclinic-I to trigonal symmetry. This transition is very similar to that described by Watkins and Corbett for the E-center (VP^0) [8]. It may be explained as the result of a thermally induced reorientation of the VH^0 defect among three equivalent orientations that have the hydrogen atom bound to the same silicon atom. The 12 equivalent orientations of VH^0 can be grouped in four sets each associated with a particular ⟨111⟩ axis, so that the members of a given set are interrelated through C_3 orientations around the ⟨111⟩ axis belonging to the set. Considering the special case of $\mathbf{B_0}$ || [111] as in Fig. 2, it is obvious that the set belonging to the [111] axis gives rise to a single line, the position of which is unaffected by the reorientation process. This line is *C* in Fig. 2. The other three sets all contribute to both line *A* and line *B*, which means that a defect reorienting at a frequency ν among the configurations within one of these sets contributes alternatingly to *A* and *B*. This switching adds a dynamic component Δω to the "static" linewidth $\Delta\omega_0$ of *A* and *B* and, since ν increases when the temperature is raised, *A* and *B* become broadened. At some temperature, ν exceeds the spectral separation ω_{A-B} between *A* and *B* causing *A* and *B* to disappear while a single line *AB* emerges at a position that is the weighted average of the original positions of *A* and *B*. This phenomenon is known as motional narrowing [14]. In the notation of Watkins and Corbett, the relationships between Δω and the lifetime τ of the reorientation process are

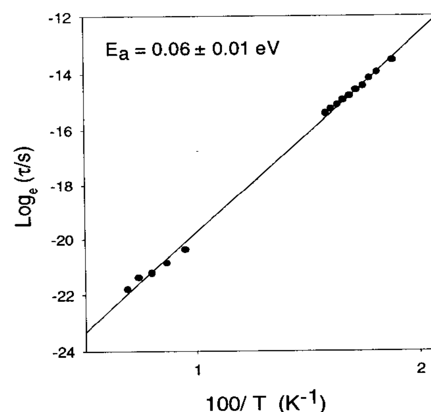

Figure 5. The temperature dependence of the lifetime τ showing that the reorientation has an activation energy of 0.06 eV.

$$\Delta\omega_A = \frac{p_A}{\tau},\quad \Delta\omega_B = \frac{p_B}{\tau}\quad \text{and}\quad \Delta\omega_{AB} = \frac{\tau}{4}\left[1-(p_A-p_B)^2\right]\omega_{A-B}^2$$

where p_A and p_B are the relative propabilities for finding the defect in a configuration contributing to line *A* and *B*, respectively (p_A = $^2/_3$ and p_B = $^1/_3$). Assuming that the lineshape is a convolution of a Lorentzian and a Gaussian [8], Δω can be estimated as $\Delta\omega = \frac{1}{2}\left(\Delta\omega_t - \Delta\omega_0 + \sqrt{\Delta\omega_t^2 - \Delta\omega_0^2}\right)$,

where $\Delta\omega_t$ is the total linewidth. From these expressions, we have estimated τ for different temperatures in the regions of broadening of *B* and narrowing of *AB*. In Fig. 5 the logarithm of τ is plotted versus T^{-1}. The simple temperature dependence $\tau = \tau_\infty \exp(E_a / kT)$ corroborates the assignment of both broadening and narrowing to a single reorientation process with an activation energy of $E_a = (0.06 \pm 0.01)$ eV. This value is exactly the same as that derived by Watkins and Corbett for VP^0 [8], which indicates that the reorientation processes in VH^0 and VP^0 are very similar.

The trigonal angular dependence of the EPR signal calculated from the g tensor measured at 45 K and the reorientation model is included in Fig. 3 as dashed curves. Noting that the linewidth is ~0.25 mT at 145 K, the agreement with the data is very good. Thus, the thermally induced symmetry change strongly corroborates our identification of the defect.

Conclusions

VH^0 is present in proton-implanted high-resistivity silicon at temperatures below 450 K. Its electronic properties are determined almost completely by the silicon dangling bond. The defect shows monoclinic-I symmetry as expected from theory, and it reorients with an activation energy of only 0.06 eV among three equivalent configurations with the hydrogen atom bound to the same silicon atom. The electronic properties of VH^0 and VP^0 are very similar, indicating that the Si-H fragment of VH^0 may be regarded as a "pseudo atom" acting like a group-V impurity.

Acknowledgements

This work was supported by the Danish National Research Foundation through Aarhus Center for Advanced Physics (ACAP).

References

[1] S.J. Pearton, J.W. Corbett, and M. Stavola, *Hydrogen in Crystalline Semiconductors*, Springer-Verlag, Berlin (1992).
[2] K. Bergman, M. Stavola, S.J. Pearton, and T. Hayes, Phys. Rev. B **38**, 9643 (1988).
[3] Yu.V. Gorelkinskii and N.N. Nevinnyi, Physica B **170**, 155 (1991).
[4] J.D. Holbech, B. Bech Nielsen, R. Jones, P. Sitch, and S. Öberg, Phys. Rev. Lett. **71**, 875 (1993).
[5] B. Bech Nielsen, L. Hoffmann, and M. Budde, Mater. Sci. Eng. B **36**, 259 (1996).
[6] P. Deák, L.C. Snyder, M. Heinrich, C.R. Ortiz, and J.W. Corbett, Physica B **170**, 253 (1991).
[7] M.A. Roberson and S.K. Estreicher, Phys. Rev. B **49**, 17040 (1994).
[8] G.D. Watkins and J.W. Corbett, Phys. Rev. **134**, A1359 (1964).
[9] S.H. Glarum, Rev. Sci. Instrum. **36**, 771 (1965).
[10] L.C. Allen, J. Chem. Phys. **40,** 3135 (1964).
[11] H. Lütgemeier and K. Schnitzke, Phys. Lett. A **25**, 232 (1967).
[12] Y.H. Lee and J.W. Corbett, Phys. Rev. B **8**, 2810 (1973).
[13] X. Zhou, G.D. Watkins, K.M. McNamara Rutledge, R.P. Messmer, and S. Chawla, Phys. Rev. B **54**, 7881 (1996).
[14] H.S. Gutowsky and A. Saika, J. Chem. Phys. **21**, 1688 (1953).